analytical chemistry

pubs.acs.org/ac Article

Sensitive Electrochemiluminescence Biosensor Based on the Target Trigger Difference of the Electrostatic Interaction between an ECL Reporter and the Electrode Surface

Yilei Lu, Xiujun Rong, Peng Wu, Jian Shou, Long Chen,* Fang Luo, Cuiying Lin,* Jian Wang, Bin Qiu, and Zhenyu Lin*

Cite This: *Anal. Chem.* 2022, 94, 5823−5829 Read Online

ACCESS | Metrics & More | Article Recommendations | Supporting Information

ABSTRACT: The discrepancy of the electrostatic interaction of negatively charged signal molecules to long and short DNA strands of the modified electrode surface has been used for the first time to the develop an electrochemiluminescence (ECL) biosensor for human papillomavirus 16 (HPV 16) DNA detection. The short single-stranded capture probe (CP) was modified first on the surface of the gold electrode, which only has a small amount of negative charge. The electrostatic interaction between the negatively charged tris(2,2′-bipyridyl) ruthenium(II) chloride hexahydrate-doped SiO_2 nanoparticles (Ru@SiO_2 NPs) and CP is weak, hence Ru@SiO_2 NPs easily diffuse to the surface of the electrode to generate a strong ECL signal. Hybrid chain reaction (HCR) amplification products (long strand dsDNA) were prepared in homogeneous solution in advance. When the target was present, the dsDNA can be connected on the electrode surface and cause the enhancement of the negative charge on the electrode surface. Owing to electrostatic interaction and steric hindrance, Ru@SiO_2 NPs are difficult to diffuse to the electrode surface, resulting in a significantly reduced ECL signal. The decrease of ECL signal is linearly correlated with the logarithm of the HPV concentration under optimal conditions, with the detection range being 0.1 fM −5 pM with a limit of 1.41 aM. This innovative methodology expands the application of electrostatic interaction in ECL sensing, but can also easily develop biosensors for detecting other targets by changing the DNA sequence used in this strategy.

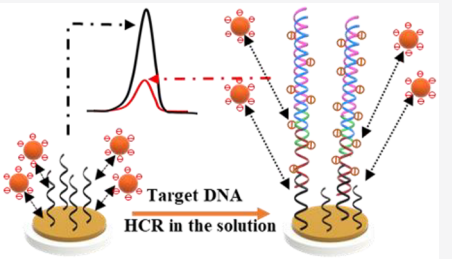

As an integration of chemiluminescence and electrochemistry, electrochemiluminescence (ECL) has the ascendancy of fast detection speed, controllability, remarkable sensitivity, and a wide linear range. Various DNA-based ECL biosensors have been designed for disease marker diagnosis.[1,2] Most of these biosensors required the immobilization of DNA primarily on the electrode interface, and then ECL reporters were modified on the electrode surface, a process that is cumbersome and causes relative low reproducibility.[3−5] Homogeneous ECL biosensors have been constructed based on the discrepancy in the electrostatic interaction between the DNA sequence of dissimilar lengths and the negatively charged indium tin oxide (ITO) electrode interface.[6−9] In these sensors, the presence of a target affects the length of the DNA strand labeled with ECL active compounds, which in turn affects the diffusion of negatively charged DNA to the surface of the electrode and causes the difference in the ECL signals recorded.[10] This technique has good reproducibility as no complex modification is needed. However, the labeling of signal molecules (ECL indicators) increases the complicacy and potentially reduces the activity of labeled biomolecules, and the low efficiency and high cost of labeling limit its wide application.[11] Subsequently, a label-free ECL aptasensor was constructed based on the different electrostatic repulsions between the ITO electrode with different dsDNAs embedded with $Ru(phen)_3^{2+}$, which has a high sensitivity and simple operation steps.[12] Nevertheless, the presence of a great quantity of free $Ru(phen)_3^{2+}$ in the solution results in a high background signal, and the embedding of the signal molecule is also time-consuming. Efforts are needed to address these problems.

Changing the amount of charge on the working electrode interface can also affect the diffusion of a charged electroactive substance to the electrode surface. This principle had been applied to develop electrochemical sensors earlier. For example, potassium ferricyanide ($[Fe(CN)_6]^{3-/4-}$) is an ordinary redox reporter group with a negative charge and is used to construct a label-free electrochemical impedance spectroscopy biosensor, which can generate different electrostatic repulsions on the DNA sequences with different lengths or densities that are modified on the electrode surface.[13,14] These methods can realize fast and label-free target detection

Received: December 5, 2021
Accepted: March 24, 2022
Published: April 6, 2022

https://doi.org/10.1021/acs.analchem.1c05258
Anal. Chem. 2022, 94, 5823−5829

Scheme 1. Scheme of the Constructed ECL Biosensor Based on the Difference in the Electrostatic Interaction for the Detection of HPV 16 DNA

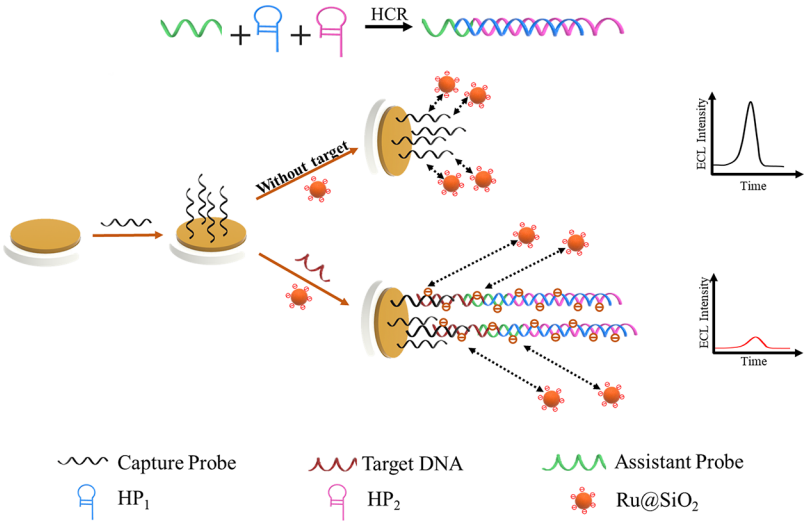

in a cost-effective manner, but they have not been coupled with a sensitive ECL detection technique.

Tris(2,2′-bipyridyl) ruthenium(II) chloride hexahydrate-doped SiO_2 nanoparticles ($Ru@SiO_2$ NPs) have been applied in ECL biosensors frequently.[15−17] The silica shell of $Ru@SiO_2$ NPs contains a large number of negatively charged silicon hydroxyl groups, which can generate electrostatic interactions with a negatively charged working electrode. In this study, this character has been used to develop a homogeneous ECL biosensor for the first time. Human papillomavirus 16 (HPV 16) E6/E7 oncogenes were selected as the model target because high-risk HPV 16 is found in 50−55% of invasive cervical cancer cases, among which HPV 16 E6 and E7 oncogenes are involved in their pathological process.[18−20] Due to the low concentration of oncogenes in actual samples, a nonenzymatic and isothermal hybridization chain reaction (HCR) has been adopted to realize signal amplification.[21] When the target sequence appears, a large amount of negatively charged HCR amplification products were captured on the electrode interface, which can amplify the change in the electrode interface charge caused by the target, thereby achieving the effect of signal amplification. The target affects the change in the electrostatic interaction between the modified electrode interface and the negatively charged nanoparticles, resulting in a weakening of the ECL signal. The decrease in the ECL signal is associated with the concentration of the target, which can realize the quantitative analysis of the target. In addition, the biosensor shows an ideal performance in detecting HPV 16 DNA in cervical brush samples. This study can also be utilized for any other DNA biomarker detection as a general platform, further expanding the application of ECL.

EXPERIMENTAL SECTION

Reagents. Triton X-100, tetraethyl orthosilicate (TEOS), 1-hexanol, cyclohexane, tris(2-carboxyethyl) phosphine hydrochloride (TCEP), tris(2,2′-bipyridyl) ruthenium(II) chloride hexahydrate ($Ru(bpy)_3^{2+}$), tripropylamine (TPA), potassium ferricyanide ($K_3[Fe(CN)_6]$), KCl, NaCl, $MgCl_2$, and potassium ferrocyanide ($K_4[Fe(CN)_6]\cdot 3H_2O$) were acquired from Aladdin Chemical Reagent Co. Ltd. (Shanghai, China). Ammonia, ethanol, acetone, and sulfuric acid (H_2SO_4) were procured from Sinopharm Chemical Reagent Co. Ltd. The 1 M Tris-HCl solution (pH = 7.4), 20× phosphate buffered saline (PBS), 5× TBE buffer, and all DNA sequences utilized in this experiment were procured from Sangon Inc. (Shanghai, China). All reagents utilized are analytically pure. Ultrapure water is applied in each process of the experiment. Sequences of oligonucleotides utilized in this work are as follows: Capture Probe (CP): 5′-CGAAATCGGTTTT-$(CH_2)_6$-SH-3′; Target: 5′-ACCGATTTCGGTTACGCCCT-3′; Assistant Probe (AP): 5′-CCCACACCCACCGCATTTCCAAGGGCGT-AAC-3′; HP1: 5′-CGGAAATGCGGTGGGTGTGGGTGA-TCGTCCACACCCACCGC-3′; HP2: 5′-CCACACCC-ACCGCATTTCCGGCGGTGGGTGTGGACGATCA-3′; HPV31: 5′-GGTGAACCGAAAACGGTTGG-3′; HPV18: 5′-GGAATGCTCGAAGGTCGTCT-3′; HPV51: 5′-TCTG-CTGTACAACGCGAAGG-3′.

Synthesis of $Ru@SiO_2$ NPs. The W/O reverse microemulsion system was preformed by mixing 7.5 mL of cyclohexane, 1.8 mL of 1-hexanol, and 1.77 mL of triton X-100. Subsequently, 680 μL of aqueous solution containing 10 mM $Ru(bpy)_3^{2+}$ was added to the above solution. Then, 60 μL of $NH_3\cdot H_2O$ and 100 μL of TEOS were added to the aforesaid solution. After stirring the reaction at room temperature for 24 h, acetone was added to separate the nanoparticles from the W/O system until precipitation no longer increases, and the orange precipitate was obtained by centrifugation at 8000 r/min for 10 min. It was rinsed with ethanol and ultrapure water three times in sequence after discarding the supernatant. Ultimately, the $Ru@SiO_2$ NPs obtained were separated in deionized water for subsequent use.

Analysis of Polyacrylamide Gel Electrophoresis. The 12% polyacrylamide gel was carried out verifying the feasibility of the designed strategy. Electrophoresis was executed at an unvarying voltage of 80 V in a 0.5× TBE buffer under room temperature for 120 min. A JS-2012 gel imager was used to photograph the electrophoresis results.

Procedures of HPV E6/E7 DNA Detection. The mirror surface of the gold electrode with a diameter of 3 mm was obtained by polishing with 0.3 and 0.05 μm Al_2O_3 powder in turn. The treated electrode was sonicated in ultrapure water for

https://doi.org/10.1021/acs.analchem.1c05258
Anal. Chem. 2022, 94, 5823−5829

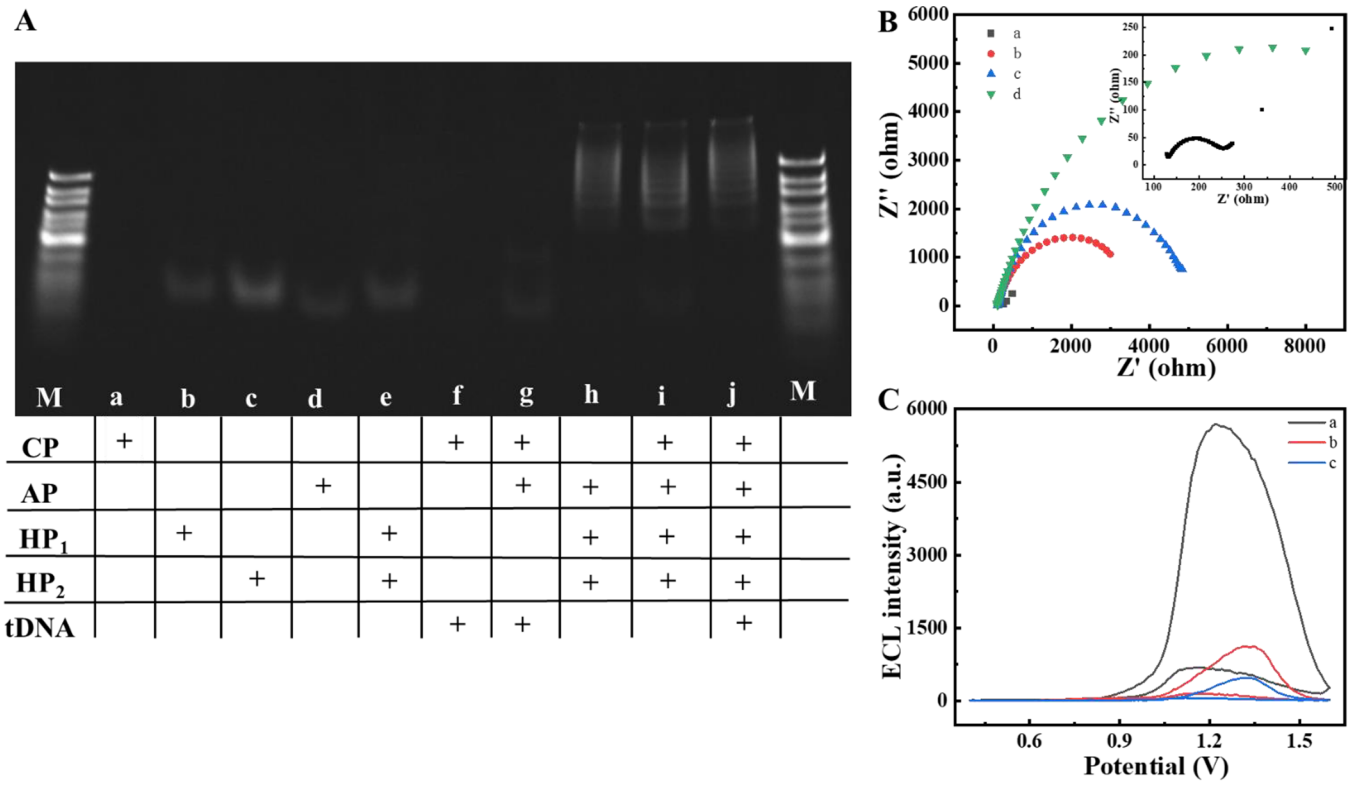

Figure 1. Viability of the constructed ECL biosensor. (A) Polyacrylamide gel electrophoresis analysis. (B) Electrochemical impedance spectroscopy of (a) bare gold electrode (b) bare gold electrode + CP (c) bare gold electrode + CP + target DNA (d) bare gold electrode + CP + target DNA + HCR. (C) ECL intensity of the constructed biosensor in the (a) bare gold electrode and in the (b) absence and (c) presence of 1 μM target DNA.

3 min and dried with nitrogen. CV measurement of the processed electrode was performed at the potential scope of −0.2 to 1.6 V and the scan rate of 100 mV/s in 0.5 M H_2SO_4 solution until a steady voltammetric peak was obtained. Afterward, the electrode surface was washed by ultrapure water and desiccated with nitrogen. Then, 0.5 μM AP, 5 μM HP1, and 5 μM HP2 were added to the centrifuge tube in equal volumes to incubate at 37 °C for 2 h to obtain HCR amplification solution, which was utilized instantly or stored at 4 °C. Subsequently, 10 μL of CP (1 μM), which was pretreated with 5 mM TCEP to reduce disulfide bonds, was introduced to the electrode surface via a Au−S bond to incubate at 37 °C for 2 h. Eventually, the modified electrode surface was immersed in 30 μL of target DNA with different concentrations, its corresponding buffer solution, and 90 μL of HCR amplification solution and incubated at 37 °C for 2 h. After each step, the electrode surface must be thoroughly washed with ultrapure water and desiccated with nitrogen.

ECL analysis was performed in 1 mL of PBS buffer containing 20 mM TPA and 2.5 μL (13.6 mg/mL) of Ru@SiO_2 NPs. The measurement was launched in the voltage scope of 0.4−1.6 V at a scan rate of 100 mV/s under the photomultiplier tube voltage of −900 V. Each electrode is measured once, and the average of the three measurement results was taken as the reference result. Error bars represent the standard deviation with three repeated mensurations.

RESULTS AND DISCUSSION

Principle of the Constructed ECL Biosensor. Scheme 1 demonstrates the principle of the designed ECL biosensor for the detection of HPV 16 E6 and E7 oncogenes. The designed hairpin DNAs (HP1 and HP2) complement each other, whereas their hybridization reaction is hindered kinetically as complementary areas being locked in the hairpin stem. The AP acts as an initiator that activates and opens the first hairpin (HP1), which instantly opens and hybridizes with the second hairpin (HP2), producing a nicked dsDNA with a ssDNA "sticky end". It further induces opening of another HP1 and triggers the continuation of the HCR procedure, eventually producing a large number of long dsDNA. When the target DNA is present, the 5′-end of the target is hybridized with the CP modified on the surface of the electrode, and the 3′-end is complemented to the AP, which connected the HCR amplification products initiated by the AP to the electrode interface. At this time, a large amount of dsDNA is modified on the electrode interface. The electrostatic repulsion and steric effect between the long dsDNA modified on the interface of electrode (contains a large quantity of negatively charged DNA phosphate skeleton) and Ru@SiO_2 NPs (the silica shell includes a large number of silicon hydroxyl groups with negative charge) make Ru@SiO_2 NPs less likely to diffuse toward the working electrode, which results in a weak ECL signal detected. When there was no target DNA in the system, HCR amplification products cannot be captured on the electrode interface. Ru@SiO_2 NPs in the solution can spread relatively effortlessly to the electrode interface, and a relatively strong ECL signal can be observed. The difference in the ECL signal detected is linearly related to the HPV concentration. Under this, a simple but sensitive ECL biosensor for target DNA detection can be developed.

Feasibility of the Designed ECL Biosensor. To certify the successful implementation of the HCR procedure, polyacrylamide gel electrophoresis was initially carried out (illustrated in Figure 1A). Lanes b, c, and d illustrate,

https://doi.org/10.1021/acs.analchem.1c05258
Anal. Chem. 2022, 94, 5823−5829

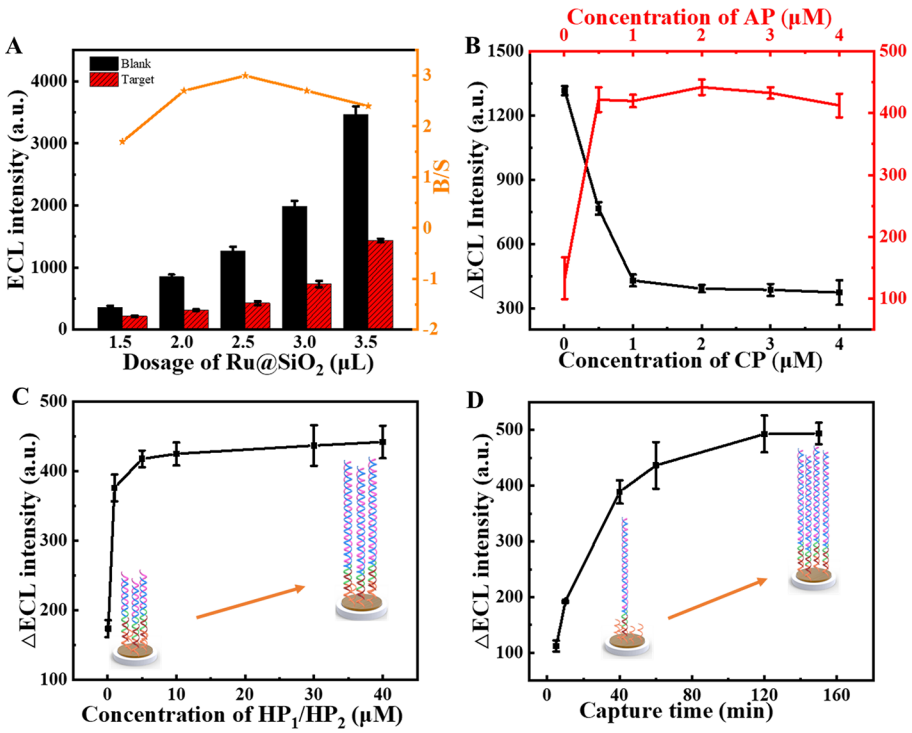

Figure 2. Optimization of different experimental conditions. (A) The influence of dosage of Ru@SiO_2 on ECL intensity. (B) The influence of CP concentration and AP concentration on ΔECL intensity. (C) The influence of HP1/HP2 concentration on ΔECL intensity. (D) The influence of HCR capture time on ΔECL intensity. The measurement was launched in the voltage scope of 0.4−1.6 V at a scan rate of 100 mV/s.

respectively, that the states of the hairpin chains HP1, HP2, and AP were in monomeric form. Lane e is the coexistent state of HP1 and HP2, which indicates that HP1 and HP2 in the solution will not open to each other. Lane h implies that HCR amplification has been triggered because there is a significant difference pattern compared to other monomer band positions when AP iss present in the system. Due to the base number of CP being negligible compared with the long chain amplified by HCR, there was no significant difference in the band positions between lane j and lane h at the existence of the target DNA, which connected CP and HCR amplified products. These consequences confirmed that the HCR amplification procedure was feasible.

Electrochemical impedance spectroscopy was applied to characterize the step-by-step modified procedure of the gold electrode. The charge transfer resistance (Ret) was equivalent to the diameter of the semicircle, which reveals the transfer kinetics of $[Fe(CN)_6]^{3-/4-}$ on the electrode interface directly. As illustrated in Figure 1B, owing to the electrostatic repulsion between $[Fe(CN)_6]^{3-/4-}$ and CP of the phosphate skeleton with a negative charge, the gold electrode modified with CP (curve b) showed a significantly higher R_{et} contrasted to the bare gold electrode (curve a), which demonstrated that the CP was modified to the electrode surface successfully via the Au−S bond. When the target DNA appears, the Ret increased slightly (curve c), indicating that the target DNA was successfully connected to the electrode surface. When the HCR amplification products were added and incubated, the R_{et} increased significantly (curve d), exhibiting that the target DNA further successfully captured HCR amplification products to the electrode surface. These results proved the successful assembly process of the gold electrode interface.

To certify the viability of the constructed ECL biosensor, the ECL experiments were further carried out (illustrated in Figure 1C). The Ru@SiO_2 NPs in the solution could freely diffuse to the bare gold electrode interface with no charge, so a strong ECL intensity could be measured (curve a). When the target DNA was absent, the ECL intensity was reduced due to the electrostatic interaction between the CP with a small amount of negative charge modified on the electrode interface and the signal molecule Ru@SiO_2 NPs (curve b). When the target DNA was existent, the target DNA could capture the HCR amplification products to the electrode interface, resulting in an increase in the amount of negative charge on the electrode interface. The ECL signal reduced significantly due to the electrostatic interaction and steric hindrance between the modified electrode surface and Ru@SiO_2 NPs. These consequences indicated that the designed biosensor can be applied to detect HPV 16 DNA.

Optimization of the Experimental Conditions. In order to obtain the finest performance of the constructed biosensor strategy for analyzing HPV 16 E6/E7 oncogenes, the dosage of Ru@SiO_2 and the concentration of CP, AP, and HP1/HP2, as well as the HCR amplification product capture time for biosensor preparation were optimized. The dosage of Ru@SiO_2 in the test solution can significantly affect the generated ECL signal (illustrated in Figure 2A). With the dosage of Ru@SiO_2 increased, the ratio of background signal to signal value (B/S) increased correspondingly and then decreased slightly. In order to achieve a better detection signal at lower background, 2.5 μL was chosen as the optimal dosage of Ru@SiO_2.

The concentration of CP modified on the gold electrode could be used to capture the HCR amplification product through the target connection and directly affected the generated ECL signal (illustrated in Figure 2B with a black line). The ΔECL intensity (the ECL intensity difference between with and without the target DNA) reached stability

https://doi.org/10.1021/acs.analchem.1c05258
Anal. Chem. 2022, 94, 5823−5829

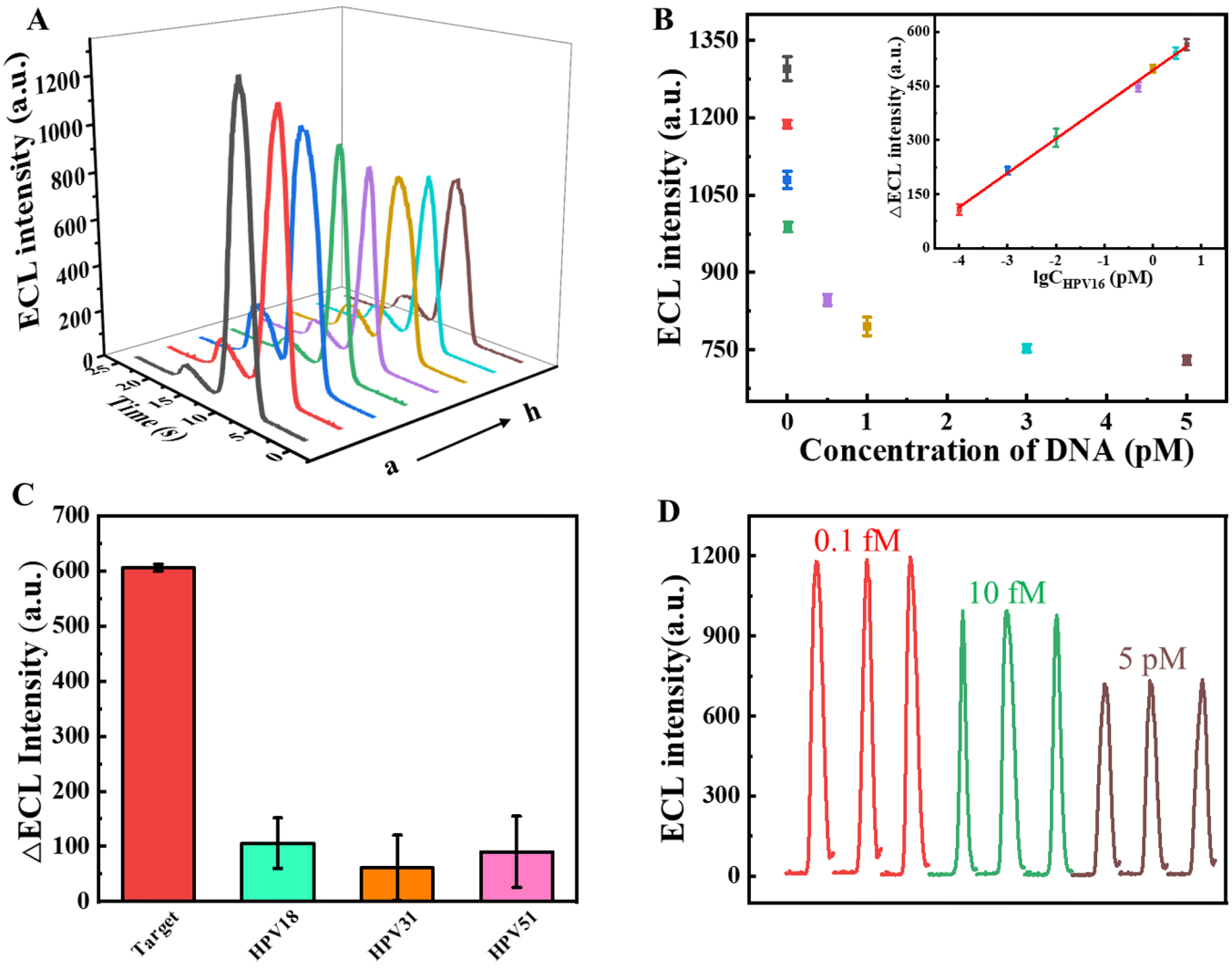

Figure 3. (A) ECL intensity of the constructed biosensor in the presence of target DNA with different concentrations (a−h: 0, 0.1 fM, 1.0 fM, 10 fM, 500 fM, 1.0 pM, 3.0 pM, and 5.0 pM, respectively). (B) Relationship between ECL intensity and different concentrations of target DNA. Inset: Linear curve of ΔECL intensity and logarithm of target DNA at different concentrations. (C) Selectivity of the proposed ECL biosensor. [HPV16] = 100 fM, [HPV18] = [HPV31] = [HPV51] = 1 pM. The error bars denote the standard deviation of three replicate determinations. (D) Reproducibility of the proposed ECL biosensor.

when the concentration of CP was 1 μM, indicating that the quantity of CP modified on the electrode surface attained saturation. Consequently, 1 μM was chosen for the following experiments. The concentration of AP had a great influence on the amplification of HCR, which affected the performance of the biosensor in turn (illustrated in Figure 2B with a red line). Accompanying the increasing concentration of AP, the ΔECL intensity was raised and reached a plateau at the concentration of 0.5 μM since the triggered HCR amplification product chain increased with the increase in the AP concentration, which further affected the amount of amplification product captured on the electrode surface. Therefore, the optimal concentration of AP was 0.5 μM.

The amount of HP1 and HP2 affects the negatively charged HCR amplification product captured by target DNA on the working electrode surface, which in turn affects the electrostatic interaction between the working electrode and the signal molecule (illustrated in Figure 2C). Accompanying the increasing concentration of HP1/HP2, the ΔECL intensity rose and tended to stabilize at 5 μM H1/H2, indicating that the charge and length of the formed HCR products are adequate to prevent Ru@SiO_2 NPs from approaching the working electrode surface.

The impact of the incubation time on the capture of HCR amplification products on the electrode interface was ultimately studied (illustrated in Figure 2D). ΔECL increases with the incubation time and levels off after 120 min, because the reaction attained saturation after a certain concentration of hairpin probes for a certain period of time. Ultimately, 120 min was chosen as the optimal capture time.

Performance of the Proposed Biosensor. The ECL response of the proposed biosensor toward target DNA with different concentrations was explored with the optimal conditions (illustrated in Figure 3A). There was a strong correlation between ΔECL intensity and target concentration displayed in Figure 3B, which illustrated that the ΔECL of the constructed biosensor was linearly linked to the logarithm of HPV 16 DNA concentration. The linear regression equation of the obtained biosensor was conveyed as

$$\Delta ECL = 94.83 \lg C_{HPV16} + 493.36, \quad R^2 = 0.9965$$

https://doi.org/10.1021/acs.analchem.1c05258
Anal. Chem. 2022, 94, 5823−5829

where C is the HPV 16 DNA concentration (pM) and R is the linear correlation coefficient. The detection range is 0.1 fM to 5 pM, and the calculated limit of detection (LOD) is 1.41 aM (LOD = $3s/k$, where the slope of the calibration curve is represented by k and the standard deviation of the blank is represented by s). The designed ECL biosensor exhibited a lower limit, higher reproducibility, and stability for the detection of HPV 16 DNA compared with other detection methods, which may be ascribed to the signal magnification effect of HCR and the high sensitivity of ECL technology (illustrated in Table 1).

Table 1. Contrast of Analytical Performance for HPV Detection with Different Biosensors

electrochemical method	linear scope	detection limit	reference
ECL	10 aM to 10 nM	6.8 aM	22
SWV[a]	10−200 nM	2.3 nM	23
ECL	0.1−200 nM	0.03 nM	24
EIS	1 pM to 1 μM	0.15 pM	25
DPV[b]	0.1 fM to 10 pM	18.6 aM	9
ECL	10 fM to 15 pM	7.6 fM	26
ECL	0.1 fM to 5 pM	1.41 aM	this work

[a]SWV: square wave voltammetry. [b]DPV: differential pulse voltammetry.

Selectivity and Reproducibility of the Designed ECL Biosensor. The specificity of the proposed ECL biosensor was evaluated under the same experimental conditions for DNA detection with different sequences containing target, HPV 18, HPV 31, and HPV 51 (illustrated in Figure 3C). The ECL intensity changes significantly after the addition of target, but it was not obvious after the addition of interference, which presumably was because only a high degree of matching sequence can connect to the electrode interface through base complementary pairing, and unmatched sequences are difficult to connect to the electrode interface and change the electrode surface charge. These consequences revealed that the proposed ECL biosensor had powerful specificity in detecting HPV 16 DNA and significant selectivity contrasted to its analogs.

The reproducibility of the ECL biosensor was studied by repeated detection of HPV 16 DNA (0.1 fM, 10 fM, 5 pM) three times (illustrated in Figure 3D). The P value valued by ANOVA is much less than 0.01, implying that the difference between the groups was significant. In addition, the calculated RSD of each group (n = 3) at the same concentration was 0.7−1.1%. The deviation within each group was small, demonstrating that the constructed ECL biosensor had a high reproducibility.

Application of the Proposed Biosensor. To further demonstrate the applicability of the designed biosensor, it was applied to HPV 16 DNA detection in clinical cervical brush sample denaturing solution. The recovery studies were performed by adding four different concentrations of target DNA (1, 10, and 100 fM) to the clinical sample solution using standard addition methods. The detection results are illustrated in Table 2. The recovery ranged from 95.9% to 105%, and the RSD was between 2.4% and 5.2% (n = 3). It demonstrated that the designed ECL biosensor was capable of being used for clinical study.

Table 2. Analysis of the Practical Application of the Designed Biosensor through Adding the HPV 16 DNA Sequence in a Clinical Cervical Brush Sample Denaturing Solution

sample No.	target DNA added (fM)	target DNA detected (fM)	recovery (%)	RSD (%) n = 3
1		24.7		4.5
	1.00	25.7	103	5.2
	10.0	35.2	105	2.7
	100	122.1	97.4	2.4
2		40.2		3.7
	1.00	41.2	102	4.4
	10.0	49.8	96.4	2.8
	100	143.0	103	3.5
3		93.8		4.3
	1.00	94.8	102	5.1
	10.0	104.3	104	2.6
	100	189.7	95.9	2.9

CONCLUSION

A sensitive ECL biosensor for HPV 16 E6/E7 oncogene detection based on the different electrostatic interactions between negatively charged signal molecules and different lengths of DNA modified on the electrode interface had been constructed. The biosensor demonstrates several captivating features: (1) The platform combines the ECL technology and the electrostatic interaction caused by the change in electrode surface charge first, which expands the application of electrostatic interaction in ECL sensing. (2) Compared with the traditional complex and expensive signal molecular labeling and time-consuming intercalation, Ru@SiO_2 was selected as the signal molecule, which is easy to synthesize and has higher luminous efficiency. (3) HCR without an enzyme and isothermal amplification is used to achieve high-efficiency signal amplification. In addition, the designability of the DNA sequence gives the proposed biosensor outstanding versatility and scalability that can be widely utilized in the design of ECL sensors for the detection of various DNA biomolecules.

ASSOCIATED CONTENT

Supporting Information

The Supporting Information is available free of charge at https://pubs.acs.org/doi/10.1021/acs.analchem.1c05258.

Additional experiment details, including the apparatus and preparation of the clinical sample, and additional figures, including the zeta potential of Ru@SiO_2 and the calibration curve between the biosensor signals and the logarithm of the kit assay results (PDF)

AUTHOR INFORMATION

Corresponding Authors

Long Chen − *Department of Obstetrics and Gynecology, Affiliated Xiaoshan Hospital, Hangzhou Normal University, Hangzhou, Zhejiang 311201, China*; Email: chenlong6517@vip.sina.com

Cuiying Lin − *Ministry of Education Key Laboratory for Analytical Science of Food Safety and Biology, Fujian Provincial Key Laboratory of Analysis and Detection for Food Safety, College of Chemistry, Fuzhou University, Fuzhou, Fujian 350116, China*; Email: lcuiying@fzu.edu.cn

https://doi.org/10.1021/acs.analchem.1c05258
Anal. Chem. 2022, 94, 5823−5829

Zhenyu Lin − *Ministry of Education Key Laboratory for Analytical Science of Food Safety and Biology, Fujian Provincial Key Laboratory of Analysis and Detection for Food Safety, College of Chemistry, Fuzhou University, Fuzhou, Fujian 350116, China;* orcid.org/0000-0001-7890-6812; Email: zylin@fzu.edu.cn

Authors

Yilei Lu − *Ministry of Education Key Laboratory for Analytical Science of Food Safety and Biology, Fujian Provincial Key Laboratory of Analysis and Detection for Food Safety, College of Chemistry, Fuzhou University, Fuzhou, Fujian 350116, China*

Xiujun Rong − *Ministry of Education Key Laboratory for Analytical Science of Food Safety and Biology, Fujian Provincial Key Laboratory of Analysis and Detection for Food Safety, College of Chemistry, Fuzhou University, Fuzhou, Fujian 350116, China*

Peng Wu − *Department of Obstetrics and Gynecology, Affiliated Xiaoshan Hospital, Hangzhou Normal University, Hangzhou, Zhejiang 311201, China*

Jian Shou − *Department of Obstetrics and Gynecology, Affiliated Xiaoshan Hospital, Hangzhou Normal University, Hangzhou, Zhejiang 311201, China*

Fang Luo − *Ministry of Education Key Laboratory for Analytical Science of Food Safety and Biology, Fujian Provincial Key Laboratory of Analysis and Detection for Food Safety, College of Chemistry, Fuzhou University, Fuzhou, Fujian 350116, China;* orcid.org/0000-0003-1480-0677

Jian Wang − *Ministry of Education Key Laboratory for Analytical Science of Food Safety and Biology, Fujian Provincial Key Laboratory of Analysis and Detection for Food Safety, College of Chemistry, Fuzhou University, Fuzhou, Fujian 350116, China*

Bin Qiu − *Ministry of Education Key Laboratory for Analytical Science of Food Safety and Biology, Fujian Provincial Key Laboratory of Analysis and Detection for Food Safety, College of Chemistry, Fuzhou University, Fuzhou, Fujian 350116, China*

Complete contact information is available at: https://pubs.acs.org/10.1021/acs.analchem.1c05258

Author Contributions

All authors are contribute to the manuscript completion. Y.L., L.C., C.L., and Z.L. participated in the conception of the experimental plan. Y.L., X.R., P.W., L.C., C.L., and Z.L. conducted experiments and collected data. Y.L., X.R., P.W., J.S., L.C., F.L., C.L., J.W., B.Q., and Z.L. analyzed and discussed the experimental data. All authors participated in the analysis and discussion of the experimental results, contributed to the writing of this article, and approved the final version of the article.

Notes

The authors declare no competing financial interest.

■ ACKNOWLEDGMENTS

This project was supported by National Sciences Foundation of China (22174018, 21974020).

■ REFERENCES

(1) Miao, W. *Chem. Rev.* **2008**, *108*, 2506−2553.
(2) Qi, H.; Zhang, C. *Anal. Chem.* **2020**, *92*, 524−534.
(3) Yao, B.; Zhang, J.; Fan, Z.; Ding, Y.; Zhou, B.; Yang, R.; Zhao, J.; Zhang, K. *ACS Appl. Mater. Interfaces* **2021**, *13*, 19816−19824.
(4) Wang, Q.; Liu, Y.; Wang, X.; Wang, F.; Zhang, L.; Ge, S.; Yu, J. *ACS Appl. Mater. Interfaces* **2021**, *13*, 25783−25791.
(5) Fan, Z.; Yao, B.; Ding, Y.; Zhao, J.; Xie, M.; Zhang, K. *Biosens. Bioelectron.* **2021**, *178*, 113015.
(6) Hou, T.; Xu, N.; Wang, W.; Ge, L.; Li, F. *Anal. Chem.* **2018**, *90*, 9591−9597.
(7) Xuan, F.; Fan, T. W.; Hsing, I. M. *ACS Nano* **2015**, *9*, 5027−5033.
(8) Chang, J.; Wang, X.; Wang, J.; Li, H.; Li, F. *Anal. Chem.* **2019**, *91*, 3604−3610.
(9) He, Y.; Cheng, L.; Yang, Y.; Chen, P.; Qiu, B.; Guo, L.; Wang, Y.; Lin, Z.; Hong, G. *Sens. Actuators, B* **2020**, *320*, 128407.
(10) Ni, J.; Lin, H.; Yang, W.; Liao, Y.; Wang, Q.; Luo, F.; Guo, L.; Qiu, B.; Lin, Z. *Anal. Chem.* **2019**, *91*, 14751−14756.
(11) Hai, X.; Li, Y.; Zhu, C.; Song, W.; Cao, J.; Bi, S. *TrAC, Trends Anal. Chem.* **2020**, *133*, 116098.
(12) Ni, J.; Yang, W.; Wang, Q.; Luo, F.; Guo, L.; Qiu, B.; Lin, Z.; Yang, H. *Biosens. Bioelectron.* **2018**, *105*, 182−187.
(13) Gao, F.; Zhang, T.; Chu, Y.; Wang, Q.; Song, J.; Qiu, W.; Lin, Z. *Microchim. Acta* **2018**, *185*, 555.
(14) Cai, W.; Xie, S.; Zhang, J.; Tang, D.; Tang, Y. *Biosens. Bioelectron.* **2017**, *98*, 466−472.
(15) Zhang, L.; Dong, S. *Anal. Chem.* **2006**, *78*, 5119−5123.
(16) Xu, C.; Li, J.; Kitte, S. A.; Qi, G.; Li, H.; Jin, Y. *Anal. Chem.* **2021**, *93*, 11641−11647.
(17) Zhang, W.; Xiong, H.; Chen, M.; Zhang, X.; Wang, S. *Biosens. Bioelectron.* **2017**, *96*, 55−61.
(18) Arbyn, M.; de Sanjosé, S.; Saraiya, M.; Sideri, M.; Palefsky, J.; Lacey, C.; Gillison, M.; Bruni, L.; Ronco, G.; Wentzensen, N.; Brotherton, J.; Qiao, Y.-L.; Denny, L.; Bornstein, J.; Abramowitz, L.; Giuliano, A.; Tommasino, M.; Monsonego, J. *Int. J. Cancer* **2012**, *131*, 1969−1982.
(19) Mittal, S.; Banks, L. *Mutat. Res., Rev. Mutat. Res.* **2017**, *772*, 23−35.
(20) Malla, R.; Kamal, M. A. *Curr. Med. Chem.* **2021**, *28*, 8163.
(21) Zhang, C.; Chen, J.; Sun, R.; Huang, Z.; Luo, Z.; Zhou, C.; Wu, M.; Duan, Y.; Li, Y. *ACS Sensors* **2020**, *5*, 2977−3000.
(22) Hong, G.; Zou, Z.; Huang, Z.; Deng, H.; Chen, W.; Peng, H. *Biosens. Bioelectron.* **2021**, *178*, 113044.
(23) Teengam, P.; Siangproh, W.; Tuantranont, A.; Henry, C. S.; Vilaivan, T.; Chailapakul, O. *Anal. Chim. Acta* **2017**, *952*, 32−40.
(24) Nie, Y.; Zhang, X.; Zhang, Q.; Liang, Z.; Ma, Q.; Su, X. *Biosens. Bioelectron.* **2020**, *160*, 112217.
(25) Karimizefreh, A.; Mahyari, F. A.; VaezJalali, M.; Mohammadpour, R.; Sasanpour, P. *Microchim. Acta* **2017**, *184*, 1729−1737.
(26) He, Y.; Liu, Y.; Cheng, L.; Yang, Y.; Qiu, B.; Guo, L.; Wang, Y.; Lin, Z.; Hong, G. *ACS Appl. Mater. Interfaces* **2021**, *13*, 298−305.